Total Environment Engineering 6 (2026) 100069

Contents lists available at ScienceDirect

Total Environment Engineering

journal homepage: www.elsevier.com/locate/teengi

Enhancing CO_2 adsorption of activated carbon via nitrogen doping: Synthesis and characterization

Elsun Azizov [a,1], Shabnam Feyziyeva [a,1], Narmina Guliyeva [c], Nizami Israfilov [a,b,*], Benoit Louis [a,*], Sergey Pronkin [a,*]

[a] CNRS, ICPEES UMR 7515, Université de Strasbourg, 25 rue Becquerel, F-67087 Strasbourg, France
[b] CNRS, CMC UMR 7140, Université de Strasbourg, 4 rue Blaise Pascal, F-67000 Strasbourg, France
[c] Department of Chemical Engineering, Baku Engineering University, Hasan Aliyev, str. 120, Baku, Absheron AZ0101, Azerbaijan

ARTICLE INFO

Keywords:
Bio-based activated carbon
Nitrogen doping
CO_2 capture

ABSTRACT

This study focuses on the rational design and synthesis of sucrose-derived nitrogen-doped porous carbon (ACN) materials for enhanced CO_2 capture. ACN were synthesized by thermochemical activation of sucrose and characterized by their specific surface area, pore size distribution, XPS analysis, and CO_2 adsorption capacities. The carbons showed excellent specific surface areas, with the best value being 2670.7 $m^2 g^{-1}$, obtained for ACN (1:1:2). Additionally, depending on the ACN, pore sizes varied between 10 Å and 37 Å. XPS analysis confirmed the successful doping of nitrogen in the carbon, as well as the presence of oxygen in the final material.

CO_2 capture analysis demonstrated that ACN (1:2:1) exhibits a superior adsorption capacity with a value of 5.8 mmol g^{-1} at 273 K and 1200 mbar despite the smallest surface area amongst materials (1431 $m^2 g^{-1}$). This study underscores the potential of carbon-based materials for CO_2 capture application, offering insights into the design principles for optimizing adsorption performance.

1. Introduction

Increasing concentration of carbon dioxide has been recognized to be the biggest driver of global warming, which leads to serious socio-economic problems (Yoro and Daramola, 2020). Therefore, developing efficient and cost-effective CO_2 capture techniques and advanced materials is the focus of contemporary numerous research efforts.

Among various CCS (Carbon capture and storage) methods, adsorption methods are considered as a potential promising option due to the several advantages, including low cost, reduced energy consumption etc. (Plaza et al., 2012). Other methods like membrane separation and cryogenic capture often require high energy input or struggle with selectivity for CO_2 in flow gas streams (Wang and Song, 2020).

Adsorption is considered to be most efficient currently available technology (Rochelle, 2009). However, absorption with liquid solvents, while effective, faces challenges of solvent degradation, equipment corrosion, and high regeneration energy demands (Buvik et al., 2021). For example, the energy demand for regenerating 35 wt. % MEA (monoethanolamine) solution, is between 3–5 GJ/t CO_2 (Zhao et al., 2017; Bravo et al., 2021). As a result, solid adsorption materials are suggested and studied to overcome those problems.

The adsorption technique is a process of selective capture of CO_2 from post-combustion gases using solid sorbents, which has advantages such as simple device, easy operation, has a high energy efficiency and regeneration possibility (Sevilla and Fuertes, 2012). When evaluating solid adsorbents, it is important to consider their surface area, density, pore size and volume, stability, and sustainability.

Nowadays, many kinds of solid adsorbent materials with porous textures, such as carbonaceous materials (Alabadi et al., 2015; Choi et al., 2009), zeolites (Zhang et al., 2019), zeolitic imidazolate frameworks (ZIFs) (Zhang et al., 2011), metal-organic frameworks (MOFs) (Israfilov et al., 2024), have been investigated for CO_2 capture performances.

Amongst these solid adsorbents, porous carbon materials have been studied intensively because of their high uptake rates (Hao et al., 2010; Wei et al., 2018; Wang and Yang, 2012), hydrophobicity, variety of form (powder, fibers, composites, sheets, tubes, etc.), and tailored surface chemistry (O, N, S, P, F or other heteroatom doping) (Hasegawa et al.,

* Corresponding authors.
E-mail addresses: nizami178@live.com (N. Israfilov), blouis@unistra.fr (B. Louis), sergey.pronkin@unistra.fr (S. Pronkin).
[1] Authors contributed equally to the paper.

https://doi.org/10.1016/j.teengi.2026.100069
Received 19 November 2025; Received in revised form 20 January 2026; Accepted 27 January 2026
Available online 31 January 2026

2015; Hulicova-Jurcakova et al., 2009; Paraknowitsch and Thomas, 2013; Sircar, 2008).

Owing to their low-cost, availability of sources, large surface area, and low energy requirements for regeneration (Li et al., 2018), carbon-based materials are considered to be one of the most promising adsorbents for capturing CO_2 (Sircar, 2008; Choi et al., 2009; Radosz et al., 2008). Some bio-sourced porous carbons have shown great potential in post-combustion CO_2 capture. For example, Deng et al. reported 5.0 mmol g^{-1} CO_2 uptake for a pine nut shell-derived activated carbon at 25 °C and ambient pressure (Deng et al., 2014).

Recently, modification of surface chemistry by nitrogen heterogeneities characterizing basic nature is recognized as a promising method for increasing CO_2 adsorption capacity (Sevilla et al., 2012; Hao et al., 2010).

For example, H. Wei et al., successfully synthesized nitrogen-doped porous carbon via a straightforward and cost-effective method. The resulting samples demonstrated prominent characteristics, including highly developed micropores, an ultra large specific surface area (3401 m^2 g^{-1}) and a high nitrogen content (4.89 at %). Their CO_2 capacity reached up to 6.0 mmol g^{-1} (at 0 °C and 1 bar) and 4.7 mmol g^{-1} (at 25 °C and 1 bar), along with high CO_2/N_2 selectivity (Wei et al., 2018).

In a separate study, Wang and Yang synthesized and compared carbon materials with varying surface areas (1361–3840 m^2 g^{-1}) and with/without nitrogen doping (6–7 wt % N). The optimized nitrogen-doped templated carbon demonstrated CO_2 capacity (4 mmol g^{-1} at 1 atm and 298 K) and selectivity (CO_2/N_2 at 1 atm = 14), while the best undoped carbon material showed a lower CO_2 capacity (3.2 mmol g^{-1} at 1 atm and 298 K). The study highlighted that nitrogen-doped templated carbon exhibited features such as fast and reversible adsorption, enhanced CO_2 capacity, improved CO_2/N_2 selectivity, thermal and moisture stability, and ease of sorbent regeneration (Wang and Yang, 2012).

In another study, L. Spessato et al. produced nitrogen-doped activated carbons (NDACs) with well-developed porosity from Brazil nut shells, KOH, and three different nitrogen-containing chemicals (TMAOH, HMTA, or MM) through a simultaneous activation-doping method. These materials exhibited high relative nitrogen surface contents (ranging from 6.40 % to 17.1 %) and substantial SBET values (ranging from 1755 to 2562 m^2 g^{-1}). Among them, AC2MM displayed the lowest SBET value (1755 m^2 g^{-1}), the highest nitrogen surface content (17.1 %), the highest pyridinic-type nitrogen group (22.99 %), and the highest CO_2 adsorption capacities (5.30 mmol g^{-1} at 273 K and 1.0 bar, and 22.60 mmol g^{-1} at 298 K and 45 bar). Additionally, the findings indicated that nitrogen doping, particularly pyridinic-type nitrogen groups (N5), played a more significant role in CO_2 adsorption compared to exceptionally high S_{BET} values (Spessato et al., 2022).

In this study, we developed a two-step synthesis process for N-doped activated carbon (ACN) from sucrose, utilizing a conventional method with KOH thermochemical activation as the final step. The aim of the study was to find optimal conditions for CO_2 adsorption by varying the concentrations of sucrose, ammonium citrate (as N-doping agent), and KOH to identify the conditions of the preparation of the best adsorbent. By incorporating the ammonium salt of citric acid, we also sought to introduce nitrogen heteroatoms into the carbon matrix of the final ACN material (Karakoç et al., 2023).

2. Experimental section

2.1. Synthesis of nitrogen modified porous carbon

The synthesis method was described in details elsewhere (Karakoç et al., 2023). Fig. 1 depicts a schematic overview of the material synthesis process, outlining essential conditions required to yield the desired final product.

This method involves multiple steps. Initially, polycondensation step occurs, where D(+)-sucrose ($C_{12}H_{22}O_{11}$, Acros Organics, 99+ % purity for analysis, CAS: 57–50–1) and anhydrous ammonium citrate ($C_6H_{11}NO_7$, Sigma, ≥97 % purity, CAS: 3458–72–8) are ground together using a coffee grinder (200 W) to ensure the uniform distribution of the reactants. The resulting powder is then placed in an oven at 160 °C under the air atmosphere for 5 h. It has been suggested (Karakoç et al., 2023) that in the presence of ammonium citrate in this step the chains of polycondensated glucose molecules are cross-linked and primary and secondary amines are incorporated in the resulting carbohydrate matrix.

Subsequently, the powdered mixture is combined with a concentrated aqueous KOH solution (Acros Organics, extra pure, approximately 85 %, flakes, CAS: 1310–58–3). The resulting semi-liquid material is subjected to drying at 130 °C for 5 h under the air. The KOH-enriched product obtained thereafter undergoes thermal activation in a tubular reactor at 800 °C for 1 hour (ramped at 10 °C/min) under a nitrogen atmosphere.

Following thermal activation, the final product is subjected to filtration successively using ultrapure water, 2 M HCl solution, and again with ultrapure water. It is then dried at 80 °C overnight for further processing. The resulting product is identified as ACN(x:y:z), where (x:y:z) denotes the mass ratios of D(+)-sucrose, ammonium citrate, and KOH, respectively. This comprehensive representation underscores the intricacies involved in producing tailored materials for various applications.

The details of synthesis of ACN are given in ESI

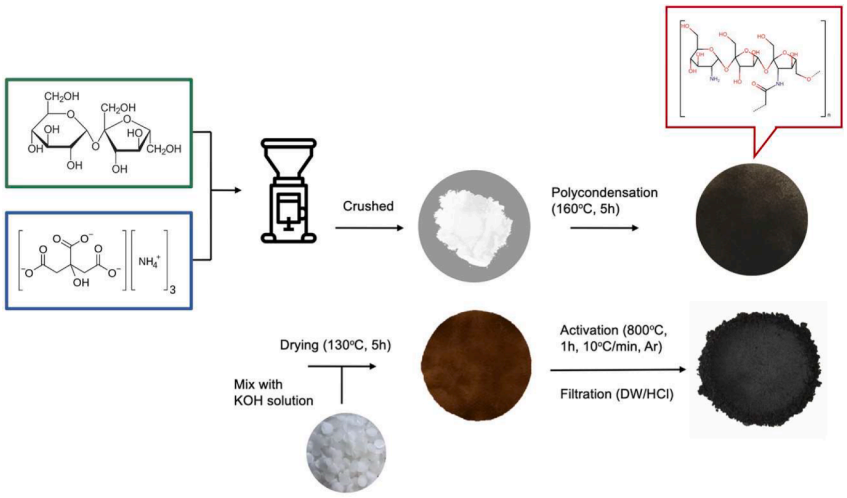

Fig. 1. Schematic illustration of the synthesis process.

2.2. BET analysis and pore size distribution

Specific surface area was determined by nitrogen adsorption–desorption measurements at 77 K using the Brunauer–Emmett–Teller (BET) method on an ASAP 2420 Micromeritics analyzer. Prior to analysis, the samples were degassed at 150 °C for 12 h. The BET surface area was calculated from the adsorption branch in the relative pressure range (P/P_o) of 0.01–1. Ultramicropore analysis was performed by CO_2 adsorption at 273 K using the same instrument and the same degassing procedure, with adsorption data collected in the relative pressure range (P/P_o) of 0.0002–0.029.

2.3. XPS analysis

X-ray photoelectron spectroscopy (XPS) analyses were performed using a Multilab 2000 Thermo Electron spectrometer equipped with an Al Kα radiation source (λ = 1486.6 eV).

2.4. CO_2 adsorption measurements

CO_2 adsorption measurements were conducted at 273 K and up to 1.2 bar using the ASAP 2420 Micromeritics analyzer, after degassing the samples at 120 °C for 2 h.

3. Results and discussions

The N_2-adsorption isotherms of ACN samples are presented in Fig. 2. SSA values were calculated from these isotherms, and listed in Table 1. The dsitribution of pore sizes calculated from adsorption isotherms of N_2 and CO_2 using NLDFT slit pores model are depicted in Fig. 3A and 3B correspondingly.

The highest surface area 2670.7 $m^2 g^{-1}$ was observed for ACN (1:1:2) sample. From the data in Table 1 it is clear that an increase in KOH quantity results in higher SSA. KOH etching of carbon at high temperatures involves several chemical reactions, which are responsible for 3 main etching mechanisms, as summarized in (Wang and Kaskel, 2012):

Etching of carbon by various potassium compounds, such as KOH, K_2CO_3, and K_2O:

$$2\ KOH \rightarrow K_2O + H_2O \quad (1)$$

$$K_2O + C \rightarrow 2\ K + CO \quad (2)$$

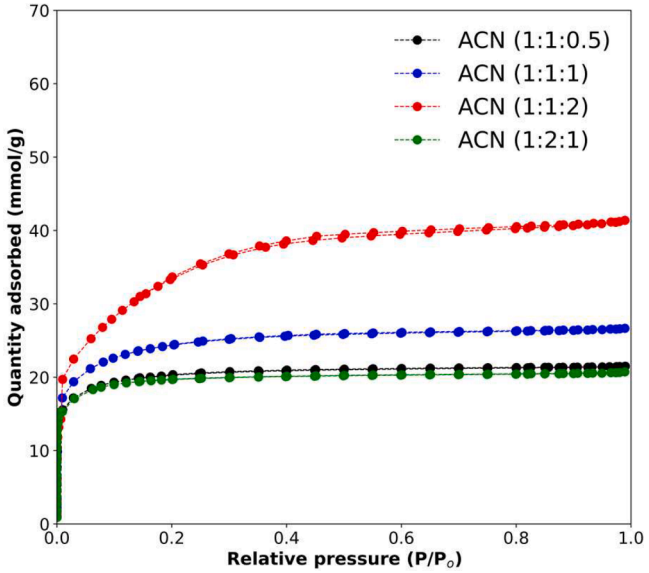

Fig. 2. Nitrogen adsorption-desorption isotherms of ACN samples.

Table 1
Structural characteristics and elementary composition of synthesized ACN materials.

	SSA (m^2g^{-1})	V_{mp} / V_p	C (at. %)	O (at. %)	N (at. %)
ACN (1:1:0.5)	1488	0.76	80.7	13	6.2
ACN (1:1:1)	1823.4	0.62	91.7	6	2.3
ACN (1:1:2)	2670.7	0.48	86.2	9.4	4.3
ACN (1:2:1)	1431	0.83	83.9	12.1	4

$$CO + H_2O \rightarrow CO_2 + H_2 \quad (3)$$

$$K_2O + CO_2 \rightarrow K_2CO_3 \quad (4)$$

Etching of carbon by H_2O and CO_2, present in the initial mixture and/or formed during the decomposition of KOH and K_2CO_3:

$$CO_2 + C \rightarrow 2CO \quad (5)$$

$$H_2O + C \rightarrow CO + H_2 \quad (6)$$

Precipitation of metallic K(formed in reaction (2)) and its intercalation into the carbon material (Romanos et al., 2012), producing (ultra-)microporosity after K is washed out in the later synthesis steps. Thus, an increase in SSA with an increase in KOH amount is expected.

An observed decrease in a relative volume of micropores (V_{mp}/V_p parameter) with an increase in KOH quantity is less expected, but in agreement with previous studies (Romanos et al., 2012). One may argue that the higher amount of gaseous CO_2 and H_2O produced from higher quantity of KOH results in widening of the pores.

It is interesting to notice that an increase in the quantity of ammonium citrate precursor have the similar effect on carbon porosity, as a decrease in KOH amount: lower SSA and higher relative micropores volume. The product of polycondensation of sucrose with citrate is expected to decompose readily at high temperature with formation of NH_3, CO_2/CO, and H_2O (Karakoç et al., 2023), resulting in stronger etching of carbon. In particular, ammonia readily reacts with disordered carbon (Jaouen et al., 2006), and in particularly with oxygen-containing carbon groups, substituting oxygen and incorporating itself into carbon matrix (Wang et al., 2010). However, despite stronger etching, lower SSA and higher V_{mp}/V_p are observed with higher quantity of ammonium citrate (sample ACN 1:2:1). In fact, this sample has lowest pore volume in the range of pore size 2–3 nm (Fig. 3A), but highest volume of ultra-micro pores with size below 0.5 nm (Fig. 3B). It has been previously reported (Karakoç et al., 2023) that the product of sucrose polycondensation in the presence of citrate has stronger cross-linking between polysacharides chains. One may argue that due to the higher stability of this precursor, the resulting carbon matrix is more resistant to etching, better conserving its microporous structure.

Table 1 presents the elemental composition of the porous carbon samples obtained from XPS analysis (see Fig.S1 for survey spectra). The table reveals the relative content of carbon, oxygen and nitrogen providing insights into their distribution within the carbon structure. Furthermore, the chemical states of carbon and nitrogen were examined through high-resolution XPS spectra, elucidating the bonding configurations and functional groups present on the surface.

According to the Table 1, the concentration of heteroatoms in carbon depends on KOH-to-carbon ratio. As discussed above, higher KOH content results in stronger etching of carbon and more defects in carbon structure, thus facilitating an interaction with N-containing intermediates and resulting higher N-doping (Pattanshetti et al., 2024). However, a decrease in N-doping with higher KOH-to-carbon precursor ratio has been also observed (Kim et al., 2020) and attributed to stronger competition with carbon etching by CO_2 and H_2O, (reactions 5, 6), especially on disordered carbons.

Pyrolysis of polycondensation precusor of ammonium citrate and sucrose by relatively low amount of KOH (sample ACN (1:1:0.5)) allows to retain high percentage of N-atoms in the structure of carbon. Increase of KOH quantity results in stronger attack of N-containing functional

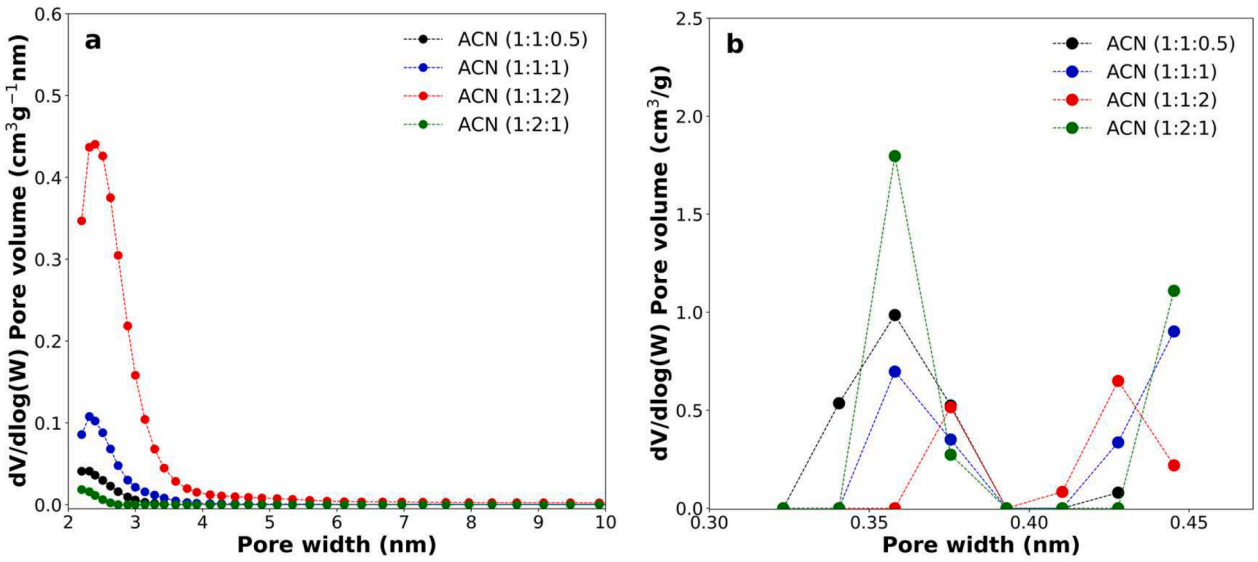

Fig. 3. Pore size distribution of ACN carbon samples.

groups and decrease in final N-doping level (sample ACN (1:1:1)). However, further increase in KOH quantity results in more defective carbon structure, which makes re-integration of N-heteroatoms in carbon structure more favorable, and leads to an increase in N-doping (sample ACN (1:1:2)).

The deconvolution of spectrum of N1s is depicted in Fig. 4, showcasing two prominent characteristic peaks that have been successfully fitted. The primary peak is observed at 400.3 eV, corresponding to the N pyrrolic (N5) group. Additionally, another peaks is discerned at 398.6 ± 0.2 eV, indicative of the pyridinic N groups (N6). Moreover, additional peaks attributed to Q-N and pyridine N oxide bonds were observed at 401.6 ± 0.2, and 403 eV (Karakoç et al., 2023; Mostazo-López et al., 2020).

The deconvolution analysis of C1s XPS spectra revealed two dominant peaks corresponding to C—C/C═C bonds at 284.7 eV and C—O bonds at 286 ± 0.1 eV. These peaks reflect the presence of sp^3/sp^2-hybridized carbon atoms and oxygen-containing functional groups in the ACN structure. Additionally, peaks attributed to C═O at 287.4 ± 0.2 eV bonds, COOH and π-π bonds were observed at 289.1 ± 0.1, and 290.9 eV, indicating the presence of carbonyl groups on the surface of ACN (Shchukarev and Korolkov, 2004; Skorupska et al., 2021).

In a similar way, the XPS O1s spectra were deconvoluted into 3 main contributions, attributed to carboxylic groups (O—C═O at 531.3 ± 0.2 eV), alkyl and ether groups (C—O at 533.2 ± 0.2 eV), and adsorbed water (H_2O at 535.2 eV).

This deconvolution demonstrates complex surface composition of ACN carbons, consisting of various O- and N-containing surface functional groups. An increase in KOH/C ratio in precursor mixture results in an increase in the presence of carboxylic and alkyl/ether groups. It can be observed that the ratio of π-π carbon bonds also increases with an increase in KOH/C ratio. One may argue that when KOH/C ratio increases, less disordered carbon remains and more O-functionalisation

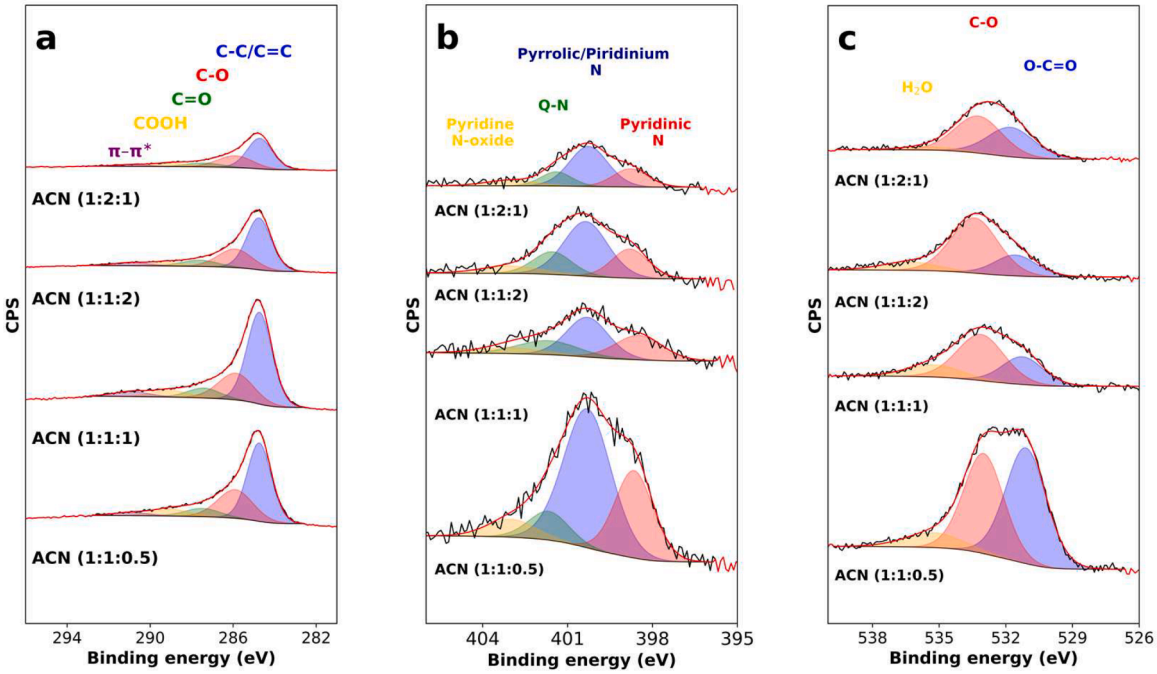

Fig. 4. XPS spectra of C1s (a), N1s (b) and O1s (c) spectra of ACN samples.

occurs due to stronger etching impact.

As it has been suggested above, an increase in ammonium citrate quantity in precursors mixture results, on the one hand, in more stable carbon matrix, and, on the other hand, in formation of higher quantity of gaseous products etching this matrix. According to XPS analysis, the latter effect results in an increase in the content of O-, and N-heteroatoms, and, in particular, of carboxylic and alkyl/ether functional groups.

The isotherms of CO_2 adsorption on ACN samples are given in Fig. 5, and the value of adsorption of 1 bar, 273 K are listed in Table 2. The sample ACN (1:2:1) show the highest and outstanding CO_2 adsorption capacity of 5.8 mmol/g.

The data of Table 2 clearly shows that high SSA of activated carbons is not a determining factor of high CO_2 adsorption. In fact, the opposite systematic trend is detected: higher CO_2 adsorption for the samples with lower SSA. There is a clear correlation between high CO_2 adsorption and high ratio of micropores volume (Table 2 and Fig.S2a). The similar correlation between the ratio of small micropores and CO_2 adsorption has been reported before (Wickramaratne and Jaroniec, 2013). It has been suggested (Sevilla et al., 2013) that for the physisorption of CO_2 on carbon the confinement of CO_2 close to the surface is crucial, and thus the micropores with size <0.8 nm are expected to be particularly efficient in CO_2 adsorption. Somewhat lower CO_2 adsorption capacity of sample ACN 1:1:1 (4.3 mmol/g) comparing to ACN 1:1:2 (4.6 mmol/g), despite its higher ratio of V_{mp}/V_p (0.60 and 0.48 correspondingly) points to the conclusion that this ratio is not the only factor to be taken into account. More favorable surface chemical composition, and namely higher content of N-heteroatoms may also play role (Table 2).

It has been discussed previously that the presence of N-heteroatoms is favorable for CO_2 adsorption (Li et al., 2020). Detailed XPS and temperature-resolved MS analysis of CO_2 adsorption of HOPG and N-doped HOPG clearly demonstrated that N-pyridinic forms CO_2 chemisorption site (Shibuya et al., 2022). However, in the case of N-doped materials with complex porous structure and surface compositions, such as activated carbons derived from bio-sources, the role of N-heteroatoms is less clear. The presence of various functional groups has to be taken into account: it has been suggested that the simultaneous presence of N- and O-heteroatoms decreases the CO_2 adsorption in comparison with only N-doped surface (Babu et al., 2017). This conclusion contradicts positive correlation between the presence of O-heteratoms and CO_2 adsorption observed in the present work (Table 2), which is related to the simultaneos influence of both

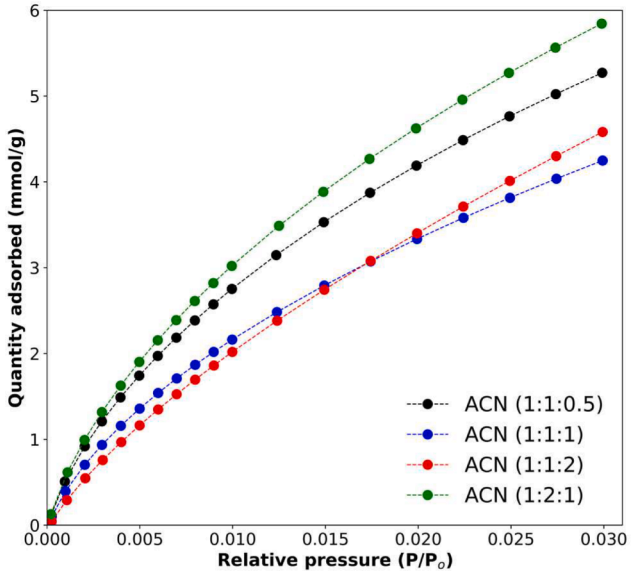

Fig. 5. CO_2 adsorption isotherms at 0 °C on ACN carbon samples.

Table 2
Properties and CO_2 uptake of various materials.

	SSA (m^2g^{-1})	V_{mp} / V_p	CO_2 (mmol/g)	T (K)	P (bar)	Ref.
ACN (1:1:0.5)	1488	0.76	5.3	273	1	This work
ACN (1:1:1)	1823.4	0.62	4.3	273	1	This work
ACN (1:1:2)	2670.7	0.48	4.6	273	1	This work
ACN (1:2:1)	1431	0.83	5.8	273	1	This work
MNC–0–800	1461	0.78	6.60	273	1	(Shi et al., 2025)
gC47	1638	0.58	5.1	298	1	(Huang et al., 2020)
GSK1–700	1636	-	7.49	273	1	(Alabadi et al., 2015)
CALF-20 MOF	528	-	4.07	273	1.2	(Roy et al., 2023), (Lin et al., 2021)
Fe@13X	734	0.71	8.59	273	1	(Xiang et al., 2023)
Mg/DOBDC MOF	1495	-	8	296	1	(Caskey et al., 2008), (Su et al., 2017)

structural parameters, namely porosity, and composition, namely presence of N- and O-containing functional groups, on CO_2 adsorption. Comparison of the CO_2 adsorption on carbon samples prepared with different amount of nitrogen precursor, often reported in the literature, is complicated as the amount of this precusor may also influence porous structure of the final material, as it has been observed in this work.

In the series of recent careful studies Shi et al. (Shi and Cui, 2024; Shi et al., 2025; Zhao et al., 2025) attempted to deconvolute the influence of porous structure and N-doping on CO_2 adsorption. For this they synthesized N-doped carbon by soft template approach either using $KHCO_3$ activation in the presence of urea (Shi and Cui, 2024; Shi et al., 2025) or gelatin as an initial precursor (Zhao et al., 2025) to control amount and nature of N-heteroatoms. Combining careful tuning of porous structure of synthesized samples, detailed XPS elementary analysis, and Monte Carlo simulation of CO_2 adsorption on heterogeneous surface, they were able to demonstrate conclusively a positive influence of pyridinic N5 nitrogen on CO_2 adsorption capacity and CO_2/N_2 selectivity. On the other hand, it has been also shown in these studies that the positive effect of N-doping is most pronounced for small pores sizes, *i.e.* for small micrpopores, and diminishes with an increase of pores sizes to meso-pores sizes. It has been also claimed (Shi and Cui, 2024; Shi et al., 2025) that the influence of pore size is more significant, comparing to the presence of N-heteroatoms. In particular, the carbon sample MNC-0–800 (Shi et al., 2025) with highest volume of ultramicropores demonstrated outstanding CO_2 adsorption of 6.60 mmol/g at 0 °C at 1 bar, despite having no N-doping.

Figs. 6a-d represent dependencies of CO_2 adsorption by carbon materials on various structural and compositional parameters, in particular on the relative content of various types of N-heteroatoms. Considering an incertitude in determination of atomic ratio of N-heteroatoms from multi-parameter deconvolution and simultaneous influence of porous structure and chemical composition, only semi-quantitative conclusions may be derived from this analysis. In particular, one may state that an increase in the ratio of micropores clearly results in higher CO_2 capacitance even for the samples with the lower total SSA. While an increase in total amount of N-doping seems to have a positive effect on CO_2 adsorption capacitance, it is predominantly related to higher content of N5 pyridinic nitrogen, in an agreement with previously reported thorough studies (Shi et al., 2025; Zhao et al., 2025). At the same time, presence of N6 pyrrolic or NQ quaternary nitrogen does not noticably improve CO_2 adsorption capacitance (Fig. 6c and d).

The results of this work also allow to suggest the positive influence of

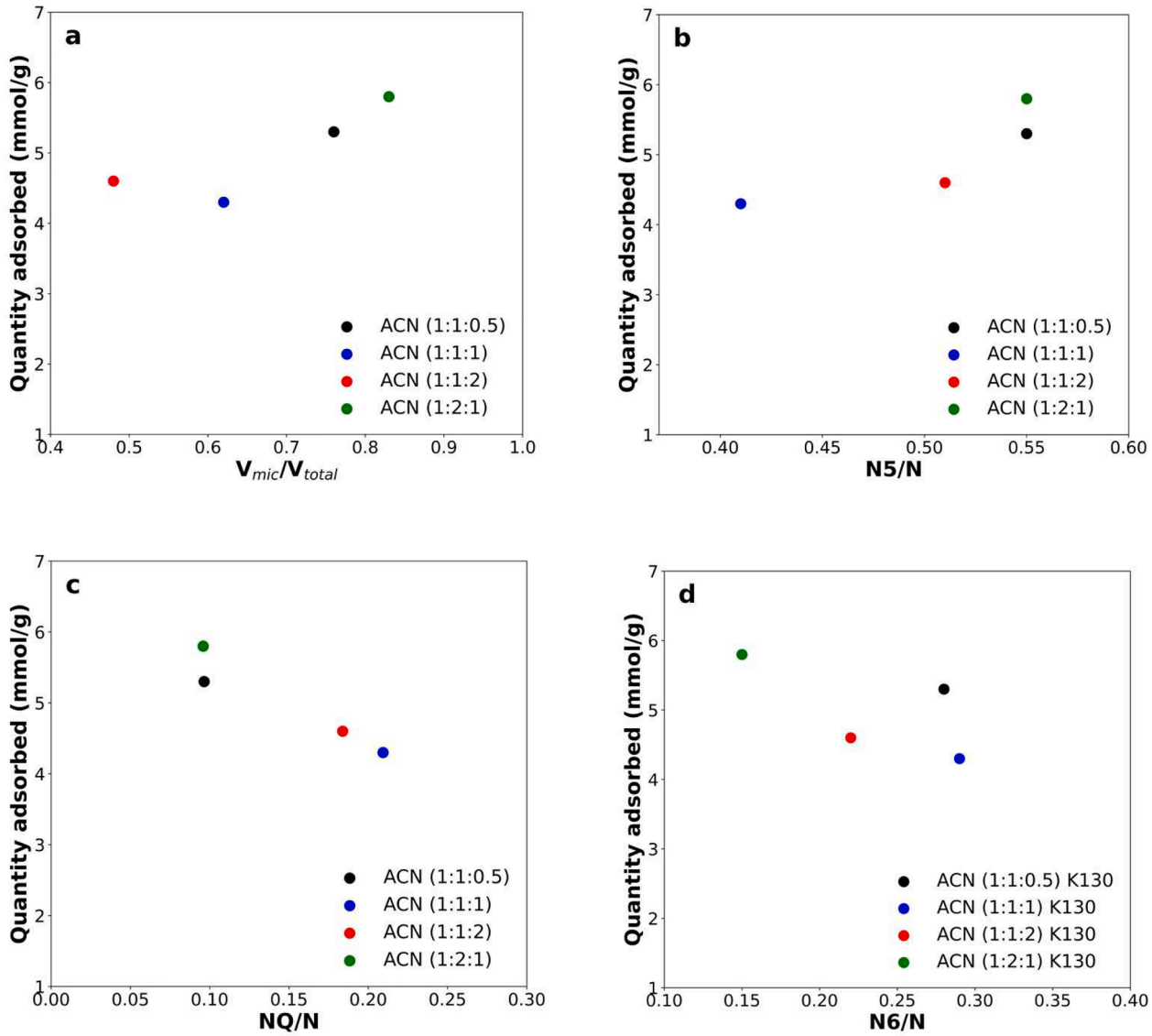

Fig. 6. Dependence of CO_2 adsorption capacity of studied samples on their ratio of micropores (a), and composition, namely, the ratio of pyridinic N5/N (b), quarternary NQ/N, and pyrrolic N6/N nitrogen to total amount of N-heteroatoms.

N-heteroatoms, in particular N-pyridinc (N5) atoms on CO_2 adsorption by carbon. However, the ratio of micropores appears to be a predominant factor determining CO_2 adsorption capacity on carbon.

4. Conclusion

Based on our initial hypothesis 4 different ACN activated carbons from sucrose with various amount of KOH and ammonium citrate were synthesized. They are fully characterized, and their CO_2 adsorption capacities were determined.

The ratio of precusors in the initial mixture strongly effects the porous structure and composition of ACN carbons. An increase in KOH:C ratio results in higher SSA and lower micropores ratio due to stronger impact of several etching reactions. The surface composition of carbon functional groups is also influenced by and increase in KOH:C ratio but in less uniform way, due to the interplay between 2 possible effects: larger quantity of etching gaseous products, and more efficient removal of disordered carbon.

An increase in ammonium citrate amount results in lower SSA and higher micropores, which is attributed to more stable carbon matrix formed from cross-linked polycondensation product between sucrose and citrate.

The ACN (1:2:1) sample synthesized with highest amount of ammonium citrate precursor shows highest CO_2 adsortpion. The CO_2 adsorption capacity correlates with micropores ratio V_{mp}/V_p, while no clear correlation between surface composition and CO_2 adsorption was detected. While positive influence of N-heteroatoms on CO_2 adsorption on carbon, often reported in the literature, is qualitatively confirmed in the case of our samples, the predominant factor determining CO_2 adsorption is the ratio of small micropores, in agreement with previous studies (Shi and Cui, 2024; Shi et al., 2025).

This study, as some previous ones (Wang and Yang, 2012; Spessato et al., 2022; Shi and Cui, 2024; Shi et al., 2025; Zhao et al., 2025) shows the applicability of carbon materials in CO_2 capture process. Their low price and high adsorption capacity makes them an interesting alternative to other materials like amine doped silicas, zeolites or MOFs.

CRediT authorship contribution statement

Elsun Azizov: Writing – review & editing, Writing – original draft, Visualization, Validation, Investigation, Data curation. **Shabnam Feyziyeva:** Visualization, Investigation, Data curation. **Narmina Guliyeva:**

Writing – review & editing, Supervision, Data curation. **Nizami Israfilov:** Writing – review & editing, Visualization, Formal analysis, Data curation. **Benoit Louis:** Writing – review & editing, Validation, Supervision, Conceptualization. **Sergey Pronkin:** Writing – review & editing, Validation, Supervision, Project administration, Data curation, Conceptualization.

Declaration of competing interest

The authors declare the following financial interests/personal relationships which may be considered as potential competing interests:

Elsun Azizov reports financial support was provided by Ministry of Science and Education of the Republic of Azerbaijan. Shabnam Feyziyeva reports financial support was provided by Ministry of Science and Education of Azerbaijan Republic. Sergey Pronkin reports a relationship with French National Research Agency that includes: funding grants. If there are other authors, they declare that they have no known competing financial interests or personal relationships that could have appeared to influence the work reported in this paper.

Acknowledgements

We thank to the Ministry of Science and Education of Azerbaijan Republic for providing scholarships for Elsun Azizov and Shabnam Feyziyeva.

Supplementary materials

Supplementary material associated with this article can be found, in the online version, at doi:10.1016/j.teengi.2026.100069.

Data availability

Data will be made available on request.

References

Alabadi, A., Razzaque, S., Yang, Y., Chen, S., Tan, B., 2015. Chem. Eng. J. 281, 606–612. https://doi.org/10.1016/j.cej.2015.06.032.

Babu, D.J., Bruns, M., Schneider, R., Gerthsen, D., Schneider, J.J., 2017. Understanding the influence of N-doping on the CO2 adsorption characteristics in carbon nanomaterials. J. Phys. Chem. C 121 (1), 616–626. https://doi.org/10.1021/acs.jpcc.6b11686.f. Jan.

Bravo, J., Drapanauskaite, D., Sarunac, N., Romero, C., Jesikiewicz, T., Baltrusaitis, J., 2021. Fuel 283, 11894. https://doi.org/10.1016/j.fuel.2020.118940.

Buvik, V., Høisæter, K.K., Vevelstad, S.J., Knuutila, H.K., 2021. Int. J. Greenh. Gas Control 106, 103246. https://doi.org/10.1016/j.ijggc.2020.103246.

Caskey, S.R., Wong-Foy, A.G., Matzger, A.J., 2008. J. Am. Chem. Soc 130, 10870–10871. https://doi.org/10.1021/ja8036096.

Choi, S., Drese, J.H., Jones, C.W., 2009. Chem. Sus. Chem 2, 796–854. https://doi.org/10.1002/cssc.200900036.

Deng, S., Wei, H., Chen, T., Wang, B., Huang, J., Yu, G., 2014. Chem. Eng. J. 253, 46–54. https://doi.org/10.1016/j.cej.2014.04.115.

Hao, G.P., Li, W.C., Qian, D., Lu, A.H., 2010. Adv. Mater 22, 853–857. https://doi.org/10.1002/adma.200903765.

Hasegawa, G., Deguchi, T., Kanamori, K., Kobayashi, Y., Kageyama, H., Abe, T., Nakanishi, K., 2015. Chem. Mater. 27, 4703–4712. https://doi.org/10.1021/acs.chemmater.5b01349.

Huang, G., Wu, X., Hou, Y., Cai, J., 2020. Biomass Conv. Bioref. 10 (2), 267–276. https://doi.org/10.1007/s13399-019-00412-6.

Hulicova-Jurcakova, D., Seredych, M., Lu, G.Q., J.Bandosz, T., 2009. Adv. Funct. Mater. 19, 438–447. https://doi.org/10.1002/adfm.200801236.

Israfilov, N., Meyer, L., Feyziyeva, S., Kyritsakas-Gruber, N., Louis, B., Planeix, J.M., 2024. J. Solid. State Chem. 332, 124582. https://doi.org/10.1016/j.jssc.2024.124582.

Jaouen, F., Charreteur, F., Dodelet, J.P., 2006. Fe-based catalysts for oxygen reduction in PEMFCs. J. Electrochem. Soc. 153 (4), A689. https://doi.org/10.1149/1.2168418.

Karakoç, T., Ba, H., Phuoc, L., Bégin, D., Pham-Huu, C., Pronkin, S.N., 2023. Batteries 9 (9), 436. https://doi.org/10.3390/batteries9090436.

Kim, J., Jeong, J.H., Ahn, H., Lee, J.S., Roh, K.C., 2020. Nitrogen-immobilized, ionic liquid-derived, Nitrogen-doped, activated carbon for supercapacitors. Chem. Electro. Chem. 7 (11), 2410–2417. https://doi.org/10.1002/celc.202000168. Jun.

Li, Z., Ma, X., Xiong, S., Ye, Y., Yao, Z., Lin, Q., Zhang, Z., Xiang, S., 2018. New J. Chem 42, 4495. https://doi.org/10.1039/c8nj00109j.

Li, Z., et al., 2020. Cost-effective monolithic hierarchical carbon cryogels with nitrogen doping and high-performance mechanical properties for CO2 capture. ACS Appl. Mater. Interfaces 12 (19), 21748–21760. https://doi.org/10.1021/acsami.0c04015. MayP. Wilson, S. Vijayan, and K. Prabhakaran, "Waste-Fish-Derived Nitrogen Self-Doped Microporous Carbon as Effective Sorbent for CO2 Capture," ChemistrySelect, vol. 3, no. 33, pp. 9555–9563, Sep. 2018.

Lin, J.-B., Nguyen, T.T.T., Vaidhyanathan, R., Burner, J., Taylor, J.M., Durekova, H., Akhtar, F., Mah, R.K., Ghaffari-Nik, O., Marx, S., Fylstra, N., Iremonger, S.S., Dawson, K.W., Sarkar, P., Hovington, P., Rajendran, A., Woo, T.K., Shimizu, G.K.H., 2021. A scalable metal-organic framework as a durable physisorbent for carbon dioxide capture. Science 374 (6574), 1464–1469. https://doi.org/10.1126/science.abi7281.

M.J. Mostazo-López, R. Ruiz-Rosas, T. Tagaya, Y. Hatakeyama, S. Shiraishi, E. Morallón, D. Cazorla-Amorós, C 6 (3) (2020), 56. https://doi.org/10.3390/c6030056.

Paraknowitsch, J.P., Thomas, A., 2013. Energy Env. Sci 6, 2839–2852. https://doi.org/10.1039/c3ee41444b.

Pattanshetti, A., Koli, A., Jadhav, V., Yu, X.-Y., Motkuri, R.K., Sabale, S., 2024. Tailoring pore architecture and heteroatom functionality of polymeric waste-derived nanoporous carbon for CO2 capture applications. Ind. Eng. Chem. Res 63 (42), 17961–17971. https://doi.org/10.1021/acs.iecr.4c02510. Oct.

Plaza, M.G., González, A.S., Pevida, C., Pis, J.J., Rubiera, F., 2012. Appl. Energy 99, 272–279. https://doi.org/10.1016/j.apenergy.2012.05.028.

Radosz, M., Hu, X., Krutkramelis, K., Shen, Y., 2008. Ind. Eng. Chem. Res 47, 3783–3794. https://doi.org/10.1021/ie0707974.

Rochelle, G.T., 2009. Science 325, 1652–1654. https://doi.org/10.1126/science.1176731, 5948.

Romanos, J., et al., 2012. Nanospace engineering of KOH activated carbon. Nanotechnology. 23 (1), 015401. https://doi.org/10.1088/0957-4484/23/1/015401. Jan.

Roy, S., Philip, F.A., Oliveira, E.F., Singh, G., Joseph, S., Yadav, R.M., Adumbumkulath, A., Hassan, S., Khater, A., Wu, X., Bollini, P., Vinu, A., Shimizu, G., Ajayan, P.M., Kibria 8, Md G., Rahman, M.M., 2023. Cell Rep. Phys. Sci. 4 (2), 2–16. https://doi.org/10.1016/j.xcrp.2023.101269, 101269.

Sevilla, M., Fuertes, A.B., 2012. J. Colloid. Interface Sci. 366, 147–154. https://doi.org/10.1016/j.jcis.2011.09.038.

Sevilla, M., Falco, C., Titirici, M.M., Fuertes, A.B., 2012. RSC. Adv. 2, 12792–12797. https://doi.org/10.1039/C2RA22552B.

Sevilla, M., Parra, J.B., Fuertes, A.B., 2013. Assessment of the role of micropore size and N-doping in CO2 capture by porous carbons. ACS Appl. Mater. Interfaces 5 (13), 6360–6368. https://doi.org/10.1021/am401423b. Jul.

Shchukarev, A., Korolkov, D., 2004. Open Chem. 2 (2), 347–362. https://doi.org/10.2478/BF02475578.

Shi, J., Xu, J., Cui, H., et al., 2024. N-doped hierarchically porous carbons prepared with the assistance of chemical blowing and in-situ hard template as highly efficient CO2 adsorbents: a combined experimental and theoretical study. Energy 294, 130892. https://doi.org/10.1016/j.energy.2024.130892. May.

Shi, J., Xu, J., Cui, H., Yan, N., Yan, R., Weng, Y., 2025. NaCl template synthesis of N-doped porous carbon from magnesium gluconate for efficient CO2 adsorption. Sep. Purif. Technol. 355, 129756. https://doi.org/10.1016/j.seppur.2024.129756. March.

Shibuya, R., Takeyasu, K., Guo, D., Kondo, T., Nakamura, J., 2022. Chemisorption of CO2 on nitrogen-doped graphitic carbons. Langmuir. 38 (47), 14430–14438. https://doi.org/10.1021/acs.langmuir.2c01987. Nov.

Sircar, S., 2008. Eds. In: Bottani, E.J., Tascón, J.M.D. (Eds.), Adsorption By Carbons. Elsevier, New York, p. 22. Ch.

Skorupska, M., Kamedulski, P., Lukaszewicz, J.P., Ilnicka, A., 2021. Nanomaterials 11 (3), 760. https://doi.org/10.3390/nano11030760.

Spessato, L., Duarte, V.A., Fonseca, J.M., Arroyo, P.A., Almeida, V.C., 2022. J. CO2 61, 102013. https://doi.org/10.1016/j.jcou.2022.102013. Utilization.

Su, X., Bromberg, L., Martis, V., Simeon, F., Huq, A., Hatton, T.A., 2017. ACS Appl. Mater. Interfaces 9 (12), 11299–11306. https://doi.org/10.1021/acsami.7b02471.

Wang, J., Kaskel, S., 2012. KOH activation of carbon-based materials for energy storage. J. Mater. Chem. 22 (45), 23710. https://doi.org/10.1039/c2jm34066f.

Wang, X., Song, C., 2020. Front. Energy Res 8, 560849. https://doi.org/10.3389/fenrg.2020.560849.

Wang, L., Yang, R.T., 2012, 116 *J*. Phys. Chem. C 1099–1106. https://doi.org/10.1021/jp2100446.

Wang, X., Lee, J.S., Zhu, Q., Liu, J., Wang, Y., Dai, S., 2010. Ammonia-treated ordered mesoporous carbons as catalytic materials for oxygen reduction reaction. Chem. Mater 22 (7), 2178–2180. https://doi.org/10.1021/cm100139d. Apr.X. Wang et al., "Nitrogen-enriched ordered mesoporous carbons through direct pyrolysis in ammonia with enhanced capacitive performance," J. Mater. Chem. A, vol. 1, no. 27, p. 7920, 2013.

Wei, H., Chen, J., Fu, N., Chen, H., Lin, H., Han, S., 2018. Electrochim. Acta 266, 161–169. https://doi.org/10.1016/j.electacta.2017.12.192.

Wickramaratne, N.P., Jaroniec, M., 2013. Importance of small micropores in CO2 capture by phenolic resin-based activated carbon spheres. J. Mater. Chem. A 1 (1), 112–116. https://doi.org/10.1039/C2TA00388K.

Xiang, X., Guo, T., Yin, Y., Gao, Z., Wang, Y., Wang, R., An, M., Guo, Q., Hu, X., 2023. Ind. Eng. Chem. Res. 62 (12), 5420–5429. https://doi.org/10.1021/acs.iecr.2c04458.

Yoro, K.O., Daramola, M.O., 2020. CO2 emission sources, greenhouse gases, and the global warming effect. In: Advances in carbon capture, Methods, Technologies and Applications, pp. 3–28.

Zhang, Z., Xian, S., Xi, H., Wang, H., Li, Z., 2011. Chem. Eng. Sci. 66, 4878–4888. https://doi.org/10.1016/j.ces.2011.06.051.

Zhang, Y., Gao, Y., Louis, B., Wanga, Q., Linc, W., 2019. J. Energy Chem. 33, 81–89. https://doi.org/10.1016/j.jechem.2018.08.014.
Zhao, B., Liu, F., Cui, Z., Liu, C., Yue, H., Tang, S., Liu, Y., Lu, H., Liang, B., 2017. Appl. Energy 185, 362–375. https://doi.org/10.1016/j.apenergy.2016.11.009.
Zhao, Ya, Cui, H., Xu, J., J.Shi, R.Yan, N.Yan, H.Guo, 2025. Synthesis of biomimetic N-doped porous carbons from gelatin using salt template coupled with chemical activation strategy for CO2 capture. Chem. Eng. J. 505, 159241. https://doi.org/10.1016/j.cej.2025.159241. February.